

Re-examination of global emerging patterns of ocean DMS concentration

Arancha Lana · Rafel Simó · Sergio M. Vallina ·
Jordi Dachs

Received: 15 March 2011 / Accepted: 1 November 2011 / Published online: 12 November 2011
© Springer Science+Business Media B.V. 2011

Abstract During the last decade the number of seawater dimethylsulfide (DMS) concentration measurements has increased substantially. The importance this gas, emitted from the ocean to the atmosphere, may have in the cloud microphysics and hence in the Earth albedo and radiation budget, makes it necessary to accurately reproduce the global distribution. Recently, the monthly global DMS climatology has been updated taking advantage of the threefold increased size and better resolved distribution of the observations available in the DMS database. Here, the emerging patterns found with the previous versions of the database and climatology are explored with the updated versions. The statistical relationships between the seasonalities of DMS concentrations and other variables are re-examined. The positive correlation previously found between surface seawater DMS and the daily-averaged climatological solar radiation dose

in the upper mixed layer of the open ocean is confirmed with both the updated DMS database and climatology. Re-examination of the latitudinal match-mismatch between the seasonalities of DMS and phytoplankton, represented by the chlorophyll *a* concentration, reveals that they are highly positively correlated in latitudes higher than 40°, but anti-correlated in the 20°–40° latitudinal bands of both hemispheres. Overall, these global emerging patterns provide key information to further understanding the factors that control the emission of volatile sulfur from the ocean. The large uncertainties associated with the methodologies used in global computations, however, call for caution in using these emerging patterns as predictive tools, and prompt to the design of time series and process-oriented studies aimed at testing the validity of the observed relationships.

Keywords Updated DMS climatology · Solar radiation dose · Mixed layer depth · Chlorophyll *a* concentration

A. Lana (✉) · R. Simó
ICM, CSIC, Barcelona, Spain
e-mail: lana@cmima.csic.es

R. Simó
e-mail: rsimo@icm.csic.es

S. M. Vallina
EAPS, MIT, Cambridge, MA, USA.
e-mail: vallina@MIT.EDU

J. Dachs
IDAEA, CSIC, Barcelona, Spain
e-mail: jordi.dachs@idaea.csic.es

Introduction

The emission of dimethylsulfide (DMS) from the ocean is the main natural source of volatile sulfur entering the atmosphere (Bates et al. 1992; Simó 2001). Once in the air, DMS oxidation products contribute to the number of small-size atmospheric

particles that are necessary for cloud formation (Andreae and Crutzen 1997). These particles influence cloud microphysics and albedo over the oceans and hence have a potential to regulate the radiation budget of the Earth (Charlson et al. 1987). The important role of DMS emissions on the radiation budget makes it necessary to accurately represent the global distribution of seawater DMS.

The DMS data coverage of the ocean is not enough to derive a reliable global distribution by direct interpolation/extrapolation of the very measurements. To be able to construct a climatology from the existing data, some kind of mapping criteria and objective analysis techniques have to be applied, and the resulting spatio-temporal distribution will carry an uncertainty inversely proportional to the number and coverage of the original data. During the last years several alternative methods for obtaining realistic global DMS fields have been proposed. Some of these are based on algorithms that derive surface DMS concentrations from other variables (Anderson et al. 2001; Aumont et al. 2002; Simó and Dachs 2002; Belviso et al. 2004), while some other are totally or partially based on numerical models (Six 2006; Bopp et al. 2008; Elliott 2009; Vogt et al. 2010). Both methods carry some uncertainties, which are mainly associated with the difficulties in the validation of the outputs, due to absence of an objective and well-covered global DMS distribution.

The DMS climatology that has been widely used hitherto was constructed a decade ago by Kettle et al. (1999; Kettle and Andreae 2000) after compiling the worldwide archived measurements of DMS concentrations in the surface ocean, i.e., at depths shallower than 10 m. The number of data available for that climatology was approximately 17,000, and were the origin of what would become the Global Surface Seawater (GSS) DMS database. Since then, the scientific community has worked hard to enlarge the database: during the last decade the number of DMS measurements has increased threefold. Following this increase, a joint initiative of the SOLAS Project Integration, COST Action 735 and EUR-OCEANS was launched to produce an updated DMS climatology (Lana et al. 2011), which is now available and posted for open access at the SOLAS Project Integration webpage (www.bodc.ac.uk/solas_integration/).

There are notable differences between the updated (hereafter L10) and the former (K00) DMS

climatologies in some regions of the ocean. The aim of this work is to re-examine in L10 some of the global emerging patterns that arose in K00 and past versions of the database and have been instrumental for better understanding the processes that regulate DMS production in the surface ocean and its emission to the atmosphere.

Methods

The seawater DMS concentration measurements used were those archived in the GSS DMS database (saga.pmel.noaa.gov/dms/) plus some additional measurements from the South Pacific (Lana et al. 2011). This database is constructed from data contributions by individual scientists and maintained at the NOAA-PMEL. In February 2011, the DMS measurements amounted 48,164 and had been collected between March 1972 and June 2010. The data submitted after the year 2000 (hereafter postK00), i.e., not used in the construction of the K00 climatology, were also analyzed in this study (24,951 DMS measurements). The updated DMS climatology (named L10) was built using the database as for April 2010 (47,313 data). Data analysis and interpolation schemes, where our current knowledge of ocean biogeochemistry and DMS variability was applied, allowed us to construct monthly gridded maps of global sea surface DMS concentrations. The objective analysis procedures, detailed in Lana et al. (2011), were essentially the same as those employed by Kettle et al. for DMS (Kettle et al. 1999; Kettle and Andreae 2000) and those used for other variables (temperature, salinity, oxygen and nutrients) in the latest version of the World Ocean Atlas (Locarnini et al. 2010) and previous editions (WOA94, WOA98, WOA01, WOA05). In brief, the first step consists of monthly gridding the historical observations into $1^{\circ} \times 1^{\circ}$ (latitude \times longitude) square means. Then, grid points were grouped according to biogeographic provinces (Longhurst 1998), DMS concentrations were monthly averaged within each province, and gradients were smoothed at province borders. The resulting global monthly maps are called the first-guess fields. These are corrected at each grid point by the difference between the observed and the first-guess value, and also by the distance-weighted mean of all the grid points with observed data that lie within the area defined by a previously

fixed influence radius. For comparative purposes, global monthly maps of surface DMS were also constructed using the algorithms of Simó and Dachs (2002), hereafter SD02, which parameterize the DMS concentration from the ratio of the chlorophyll *a* concentration (Chla) and the mixed layer depth (MLD). We recomputed SD02 using a SeaWiFS Chla climatology for the years 1997–2009, and the MLD climatology re-calculated from de Boyer Montégut et al. (2004) as in Vallina and Simó (2007a).

In all computations, DMS and Chla data were constrained within the 99.95 percentile. This way we wanted to avoid very high DMS and Chla values associated with very localized hotspots or potentially created by sampling and handling artifacts, which might have a disproportionate weight in global distributions. This imposed an upper limit of 220 nM for the GSS DMS data, 148 nM for the postK00 data, 34 nM for the L10 climatology, 95 nM for the K00 climatology, and 59 nM for the SD02 parameterization output. The upper limit for Chla was 10 mg m^{-3} .

To re-examine the proposed proportionality found between DMS and the solar radiation dose (SRD) over most of the global surface ocean (Vallina and Simó 2007a, hereafter VS07), and assess the influence that the increased number of data has had on it, we computed the daily-averaged solar radiation in the upper mixed layer as in VS07, i.e., by: (a) calculating the solar irradiance at the top of the atmosphere (Brock 1981), (b) converting it into ocean-surface irradiance by a reduction by a half (Kiehl and Trenberth 1997), and (c) calculating the mean solar radiation in the mixed layer using a constant underwater light extinction coefficient (0.06 m^{-1}) and the aforementioned climatology of the MLD. Monthly DMS concentrations and SRD were averaged by boxes of either $10^\circ \times 20^\circ$ (latitude \times longitude), as in the original study by VS07. Monthly box DMS data were then paired with monthly box SRD data for regression and correlation analyses. We imposed an upper limit of 10 nM for the 10° latitude– 20° longitude box DMS averages (95 percentile) to avoid ephemeral patches of high DMS levels associated with eutrophic coastal systems and constrain the analysis into the large majority of the open ocean, also to compare to the original study.

An alternative calculation of the SRD was also done, with the incorporation of the following computations: (a) the conversion of the solar irradiance at the top of the atmosphere into ocean-surface irradiance

was done taking into account the variable influence of clouds on reducing surface irradiance. To this aim, a cloud albedo climatology for the period 2001–2009 was obtained from CERES (Cloud and Earth's Radiant Energy System). At each $1^\circ \times 1^\circ$ pixel, the daily irradiance at surface was computed as: $\text{EDAY}_{\text{surf}} = (\text{EDAY}_{\text{toa}} \times (1 - \text{ALB}_{\text{toa}})) \times 0.72$. Where EDAY_{toa} is the shortwave irradiance at the top of the atmosphere, ALB_{toa} is the cloud albedo at the top of atmosphere, and 0.72 is the average sunlight transmittance of a clear-sky atmosphere. (b) The mean solar radiation in the mixed layer depth was calculated using the computed $\text{EDAY}_{\text{surf}}$ and a climatology of the estimated underwater light extinction coefficient (at 490 nm) provided as an ocean colour product by the SeaWiFS Project.

Global maps of seasonal correlations were created with the following procedure (Vallina et al. 2007): using a running window of $7^\circ \times 7^\circ$, we obtained for each position ($1^\circ \times 1^\circ$ pixel) of the global ocean a time series of 12 points (months) for paired of the two variable's data to compare. Each of the 12 points of the time series is the average of the 49 values taken by the pixel-centred running window in a given month. Then, for every $1^\circ \times 1^\circ$ grid box of the global ocean we calculate the seasonal Spearman correlation coefficient (ρ) between the two variables (12 degrees of freedom), generating a global map of seasonal correlations. Correlations were significant at 95% confidence level for $|\rho| > 0.5$.

To re-examine the extent of the connection between the DMS concentration and sea surface microbiota (Vallina et al. 2006), we used L10 and the monthly SeaWiFS Chla climatology derived from 1997 to 2009 data, and evaluate the global map of seasonal correlation. Regression and correlation analyses were also performed with monthly DMS and chlorophyll *a* concentration data averaged by boxes of $10^\circ \times 20^\circ$ (latitude \times longitude).

Results and discussion

Global DMS distributions

Five representations of the global distribution of surface seawater DMS concentrations are compared by means of Hovmöller, latitude versus month diagrams (Fig. 1). The subplots correspond to the

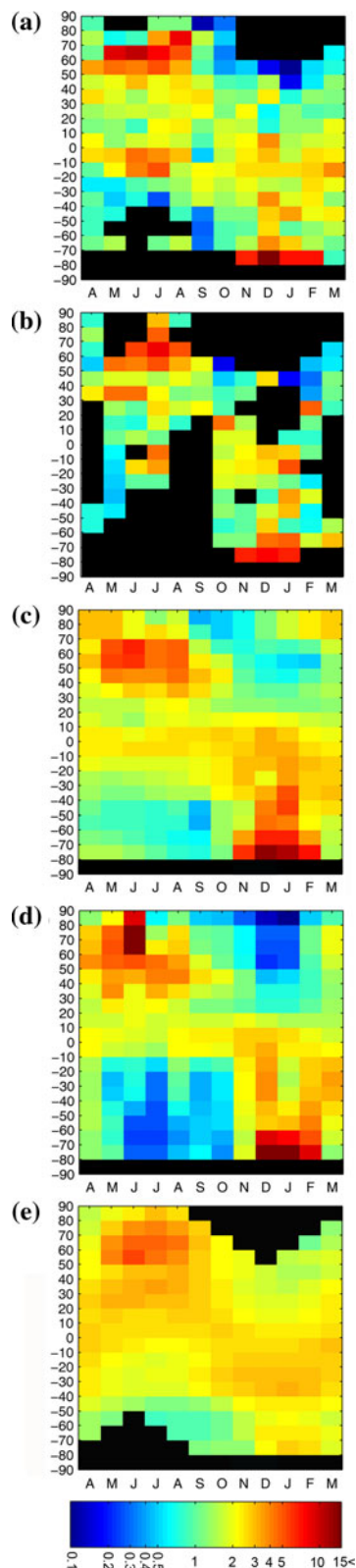
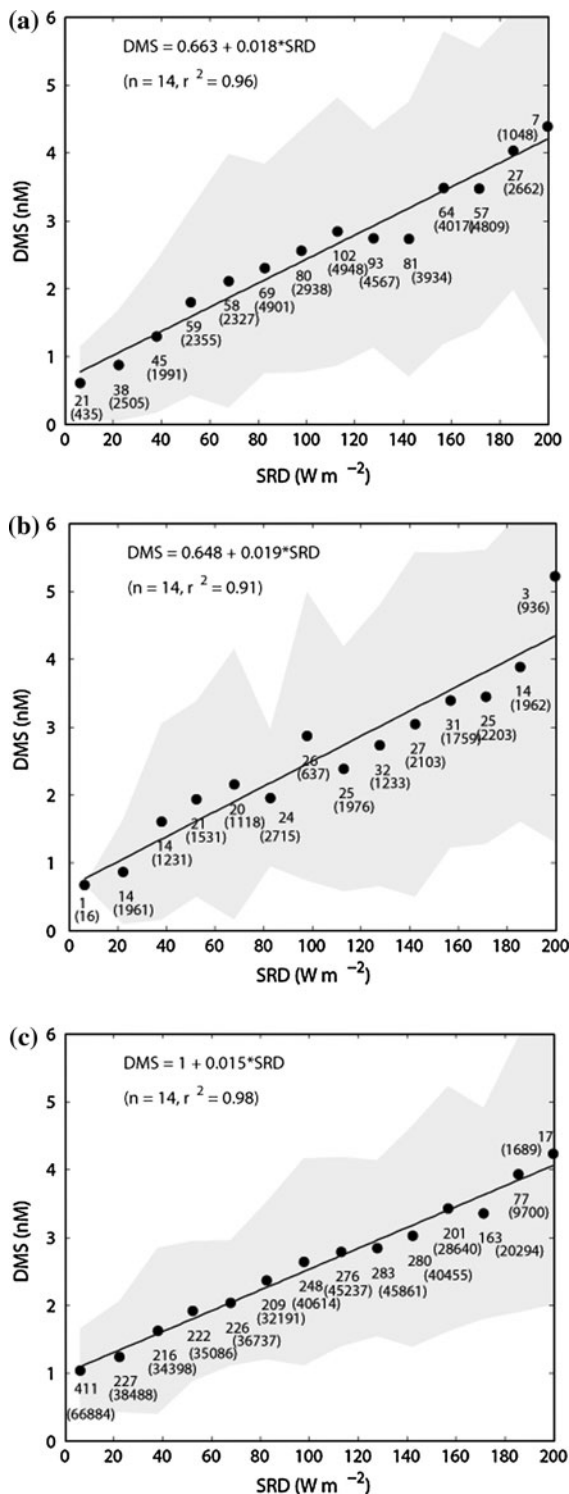


Fig. 1 Monthly averages by 10° latitude bands of **a** Surface DMS seawater concentrations (GSS DMS database), **b** Surface DMS seawater concentrations from the GSS DMS database after the year 2000, **c** updated DMS climatology L10 (Lana et al. 2011), **d** DMS climatology K00 (Kettle and Andreae 2000), and **e** DMS distribution using SD02 algorithm (Simó and Dachs 2002)

GSS DMS data distribution (Fig. 1a), with their associated gaps, the postK00 data (Fig. 1b), with a higher number of gaps due to the reduced number of data, the two representations of the L10 and K00 climatologies (Fig. 1c and d), and the distribution produced with the global SD02 parameterization (Fig. 1e), with winter gaps at high latitudes reflecting lack of satellite Chla concentrations. The GSS data (total and after 2000), the two climatologies and the parameterization all show increased DMS concentrations at mid and high latitudes during the hemispheric summer months. In most cases, the maximum annual values for all 10° latitudinal bands are ≤ 15 nM.

As reported and discussed in Lana et al. (2011), the almost three fold increase in the number of data between K00 and L10 resulted in some remarkable differences in the climatologies despite the large similarity in the general pattern. K00 predicted much higher DMS concentrations than L10 in the high latitudes ($\geq 65^\circ$) in both hemisphere summers, whereas the situation is reversed in the 40° – 60° bands. In the tropical/subtropical latitudinal bands (10° – 40°), L10 predicts smoother seasonal patterns where K00 depicts larger differences between summer and winter. This is particularly so in 10° – 40° S, and may be due to data inclusion in regions (South Indian Ocean and the Pacific Warm Pool) that were severely undersampled 10 years ago. Most of the months of the year have data in that particular band in the updated database, due to the data submitted after the creation of the K00 climatology (see Fig. 1b). Relatively high values can be observed in that latitudinal band for the GSS updated data (Fig. 1a) and the postK00 data distribution (Fig. 1b).

Interestingly, the SD02 parameterization, whose algorithms were derived from the same data as K00, predicts seasonal patterns more similar to L10 than to K00 in the lower latitudes. These regions are a large part of the ca. 80% of the global ocean where the algorithm used to calculate the DMS concentration depends only on the MLD (Simó and Dachs 2002). This further supports the suggested fundamental role



the MLD plays in controlling monthly surface DMS concentrations, through its effects either on plankton dynamics or on the solar radiation entering the mixed

◀ **Fig. 2** Linear regression against the Solar Radiation Dose (SRD) of the seawater DMS concentrations averages of 10° latitude by 20° longitude boxes, binned by SRD intervals of 15 W m^{-2} ; DMS data are obtained from: **a** updated GSS database; **b** data after the year 2000 from GSS database; **c** DMS climatology L10. The shaded area represents the standard deviations (accounting for approximately the 66% of the data set)

layer, or both (Simó and Pedrós-Alió 1999; Vallina and Simó 2007a). In general, though, SD02 generates global monthly distributions that are more homogeneous than any of the climatologies, and fails at capturing the high summer DMS concentrations south of 60°S . As pointed out by Halloran et al. (2010), empirical parameterizations that are based on the knowledge of DMS production, such as SD02, should be appropriate to simulate present distributions of global DMS. However, they should be used with care as predictive tools in Earth-System models.

DMS versus SRD

To re-assess the global relationship between DMS and SRD reported by Vallina and Simó (2007a), we followed the same approach. We grouped the DMS data of either the GSS database, the postK00 data or the L10 climatology into boxes of 10° latitude \times 20° longitude, and the same grouping was also applied to the SRD data. Box averages were calculated for each month, and the DMS averages were further grouped according to SRD bins of 15 W m^{-2} . Binned DMS means and standard deviations (accounting for approximately the 66% of the data set) are plotted against the corresponding SRD bins in Fig. 2a, b and c, which correspond to the GSS DMS database, GSS DMS data measured after the year 2000, and L10, respectively. Analyzed this way, climatological SRD accounted for 96% of the variance of monthly regional surface DMS concentration in the GSS database, 91% for the postK00 data and 98% in L10. This confirms and even reinforces the findings of VS07. As in the previous study, standard deviations are quite large but the upper and lower contours of the scatter still show clear proportionality between DMS and the SRD.

As shown in Fig. 3, the use of an alternative calculation to obtain the SRD produces changes in the statistical relationship between DMS and SRD. This alternative approach to the computation of the SRD includes the cloud albedo in the calculation of surface

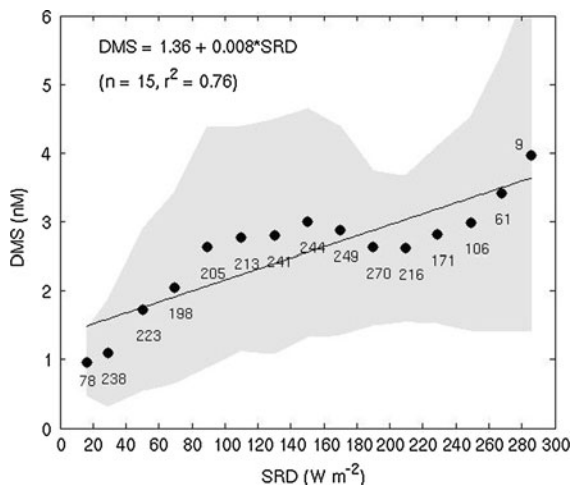


Fig. 3 Linear regression against the alternative calculation of Solar Radiation Dose (SRD) of the seawater DMS concentrations values obtained from L10 climatology, averages of 10° latitude by 20° longitude boxes, binned by SRD intervals of 20 W m^{-2}

irradiance from the top-of-atmosphere insolation, and a satellite-derived parameterization of the underwater light extinction coefficient—see “Methods”. The L10 climatology and the alternative SRD were grouped into $10^\circ \times 20^\circ$ boxes, and the DMS was averaged according to 20 W m^{-2} SRD intervals. The regression coefficient is notably reduced, to a value of 0.76. Not only the metrics show a worse coupling, also the shape of the curve indicates linearity is notably lost and there seems not to be proportionality of DMS to SRD at intermediate SRD values (Fig. 3). This poses some question mark on the otherwise linear relationship observed with either calculated climatological SRD with fixed atmospheric and underwater attenuation values, or with in situ DMS and SRD at two subtropical sampling sites (Vallina and Simó 2007a). The objective of calculating SRD with inclusion of the cloud albedo was to account for regions of persistent cloudiness where the 50% atmospheric reduction of irradiance falls short (e.g., the Pacific intertropical convergence zone). It has to be noted, however, that the cloud albedo used is nothing but a climatology, and that for the most of the marine atmosphere cloudiness is very variable. The subsequent calculation of the atmospheric reduction is an approximate parameterization, and the same applies to the underwater light attenuation based on satellite measurements. Pretending these computations will show a more realistic

relationship against non-contemporaneous DMS concentrations is almost as risky as the simple approach previously used.

The use of binned correlations between box averages is justified by the fact that the DMS data correspond to a combination of 40 years of measurements, and the SRD data are obtained with a climatological calculation. That is, DMS and SRD data are not contemporaneous and therefore they are not expected to be closely linked over a $1^\circ \times 1^\circ$ grid. With the aim at exploring to what extent climatological DMS concentration responds in proportionality to climatological SRD in the upper mixed layer, we apply a binning to reduce (smooth out) small scale variability and extract first order processes from the noisy data obtained with different spatial and temporal resolution. VS07 chose a binning interval of 15 W m^{-2} , which roughly is the range of SRD variation from month to month at mid latitudes. However, Derevianko et al. (2009) have noted that the use of box grouping and binning largely reduce the total variance in the data and result in exaggeratedly high coefficients of determination.

The window (or box) size we first used here is the same as that in VS07 because we wanted to compare the results. We further changed the size to evaluate its effect on the regression between SRD and DMS. We repeated the analysis with boxes of $7^\circ \times 7^\circ$, $5^\circ \times 5^\circ$ and $1^\circ \times 1^\circ$, always with a SRD binning interval of 15 W m^{-2} . The results show very similar regression coefficients. For the L10 climatology there is almost no variation in the regression coefficients for different windows. The GSS database had a regression coefficient reduced to 0.86 when the windows were $7^\circ \times 7^\circ$, but recovered (0.95) with $5^\circ \times 5^\circ$ windows. The DMS values obtained after the year 2000 showed more variable correlation coefficients against the SRD with changes in the window size: 0.82 for windows of $7^\circ \times 7^\circ$, 0.87 for $5^\circ \times 5^\circ$ and 0.96 for $1^\circ \times 1^\circ$. According to these results and those of Derevianko et al. (2009), the binning interval seems to have higher influence than the box averaged sizes in the correlation coefficients between DMS and SRD.

It can be argued that even a smaller window, or a narrow-range binning does not provide a realistic assessment of the co-variation between variables, and that direct correlation of gridded data or boxes would be more appropriate. VS07 reported a Spearman's rank correlation coefficient of 0.47 for the monthly

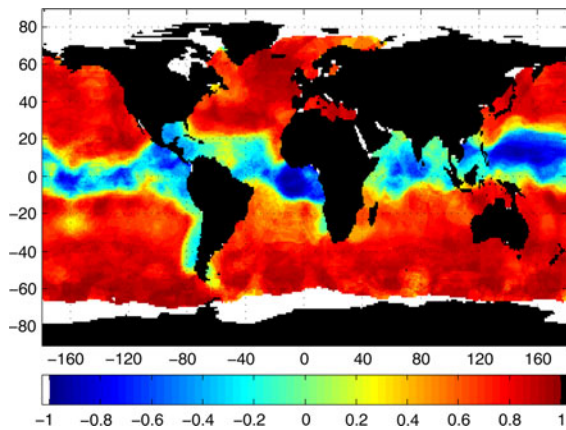


Fig. 4 Global distribution of Spearman's rank coefficients of correlation between monthly series of DMS (updated climatology L10) and the alternative Solar Radiation Dose

$10^{\circ} \times 20^{\circ}$ boxes of the GSS database DMS and the SRD ($n = 545$). Using the latest version of the database, this coefficient becomes 0.45 ($n = 806$). After noting that the DMS concentrations do not follow a normal distribution, Lana et al. (2011) computed the correlation between the $1^{\circ} \times 1^{\circ}$ gridded, log transformed climatological DMS and SRD data, and obtained a Pearson's correlation coefficient of 0.58 ($n = 452,269$). All these statistics, which are significant with a probability $>99.99\%$, suggest a certain degree of proportionality between DMS and SRD on a global scale.

For the sake of a further comparison between DMS and the alternative SRD, a global correlation map (Fig. 4) was calculated using the updated DMS climatology, L10. The Spearman's correlation map shows that there is a strong seasonal coupling between both variables all over the global ocean. The seasonal coupling is broken in the equatorial area. We still do not have a sound explanation for the equatorial exception, but it has to be noted that seasonality is very weak around the equator. Negative or low correlation values may be produced by the low seasonality, since any uncertainty in the distribution of DMS may easily have a larger amplitude than the seasonal pattern.

Mechanisms behind the emerging pattern of proportionality between DMS and SRD, yet not fully resolved, are related to photobiological effects on DMS producers and consumers, and photophysical effects on the hydrodynamics of the upper ocean, and

have been discussed elsewhere (Simó 2004; Toole and Siegel 2004; Vallina and Simó 2007a, b; Vila-Costa et al. 2008). A recent study by Galí et al. (2011) has shown that the exposure to solar radiation, UV included, increases gross DMS production, confirming sunlight as an important modulator of DMS. However, we have also shown that the relationship between climatological SRD and DMS data is influenced by the calculation of the SRD and the use of different DMS climatologies. Miles et al. (2009) used exclusively in situ data of irradiance and attenuation coefficient to calculate in situ SRD and compared them with DMS measurements in the Atlantic Ocean (they showed that, although DMS and light were significantly correlated, the correlation value was increased if they replace the in situ by climatological data for the calculation of SRD). Further studies should address this issue based solely on contemporaneous in situ measurements throughout seasons; only this way we will be able to evaluate the potential response of DMS production and emission to solar radiation, which is a required component of the hypothesized negative feedback that would link ocean biosphere and climate through atmospheric sulfur (Charlson et al. 1987).

DMS versus Chla

Global $1^{\circ} \times 1^{\circ}$ maps of correlations between monthly DMS (K00 and L10) and Chla climatology concentrations are shown in Fig. 5a and b. Seeing DMS as a biogenic trace gas, some degree of proportionality of its concentration to that of Chla (a commonly used measure of phytoplankton biomass) has often been sought, with success only at the regional scale but not at the global scale (Kettle et al. 1999; Lana et al. 2011). Figure 5a and b show that, globally, a match-mismatch between the seasonalities of the two variables occurs largely depending on latitude: north of 40°N and south of 40°S , DMS shows a strong positive correlation to Chla, whereas in the 10° – 40° latitudinal bands of both hemispheres the relationship reverses into anti-correlation. This latitudinal distribution of correlations obtained with K00 (Fig. 5a), and already reported by Vallina et al. 2006, occurs also with L10 (Fig. 5b). It is remarkable how abrupt the transition is between positive and negative correlations at around 40° in both hemispheres. This is coincident with the upper latitudinal boundaries of the major subtropical ocean gyres.

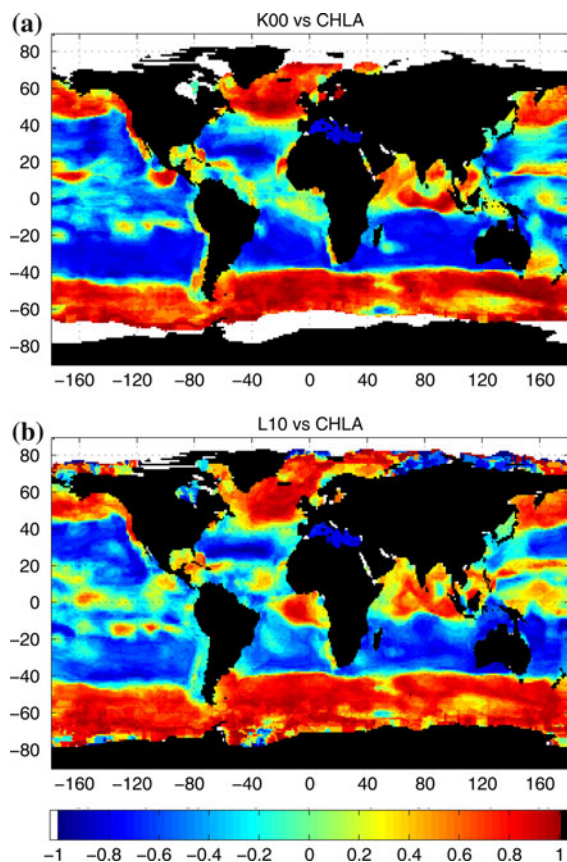


Fig. 5 Global distribution of Spearman's rank coefficients of correlation between monthly series of Chla concentrations (SeaWiFS climatology of the years 1997–2009) and **a** DMS (climatology K00) and **b** DMS (updated climatology L10)

The coincidence of the annual maxima of DMS concentrations with minima of phytoplankton biomass in subtropical and low temperate regions, where the stratification season is long and primary production is essentially limited by nutrient availability, has been called the 'summer DMS paradox' (Simó and Pedrós-Alió 1999), and has been attributed to a combination of plankton community succession and the effects of sunlight on plankton (Dacey et al. 1998; Simó and Pedrós-Alió 1999; Stefels 2000; Sunda et al. 2002; Simó 2004; Toole and Siegel 2004). This feature is difficult to reproduce with numerical models (Le Clainche et al. 2010). The production of the microalgal metabolite dimethylsulfoniopropionate (DMSP) seems to have much to tell about this paradox. DMSP is the main biogenic precursor of DMS in the ocean. One of the intracellular functions of DMSP in algal cells is as photoprotector. At some specific areas

DMSP concentrations correlate with photo-protective pigments, instead of with chlorophyll *a* concentration (Bell et al., 2010). Hence the correlation between chlorophyll *a* and DMSP is broken for those areas, and so is expected to be for DMS too. It has to be noted, though, that an important time lag between the annual maxima of DMSP and DMS has been reported in the subtropical waters of the Sargasso Sea (Dacey et al. 1998) and the Mediterranean (Vila-Costa et al. 2008). The key to the understanding of the 'summer DMS paradox' is not to be found only in the understanding of the association of DMSP to phytoplankton ecotypes. Further studies of the multiple paths and players involved in determining the efficiency of the DMSP-to-DMS conversion at the community level are needed.

At high latitudes, conversely, where the stratification season is shorter and primary production is limited or co-limited by light, both phytoplankton and DMS peak in summer (Vallina et al. 2006; Kiene et al. 2007).

Differences between L10 and K00 with respect to their respective correlations to Chla occur in the equatorial Indian Ocean and in the eastern equatorial Atlantic. These areas, where there is less correlation with the K00 climatology (Fig. 5a), confirming the results found with a different Chla climatology (Vallina et al. 2006), show a strong positive coupling with L10 (Fig. 5b). In the equatorial and northern Indian Ocean, both phytoplankton biomass and DMS increase in phase in June through September at the pace dictated by the monsoons. In the northwest sector, this is due to the southwest monsoon wind (Dasgupta et al. 2009); in the equatorial sector, high Chla levels come associated with the heavy precipitations of the monsoons, which transport silt and nutrients from land to sea through the rivers (Dasgupta et al. 2009). In the eastern equatorial Atlantic off the coasts of Africa, DMS also appears to peak in the period from June to September, yet this seasonal pattern is largely uncertain due to a severe lack of data (Lana et al. 2011). Water discharges by the Congo River, added to the direction of the South Equatorial Current, seem to be the causes of higher Chla levels in the same period (Dasgupta et al. 2009).

The same regression analysis used with L10 and the SRD was applied to the Chla climatology. Both L10 DMS and Chla data were averaged by $10^{\circ} \times 20^{\circ}$ boxes, and the box DMS means were plotted against

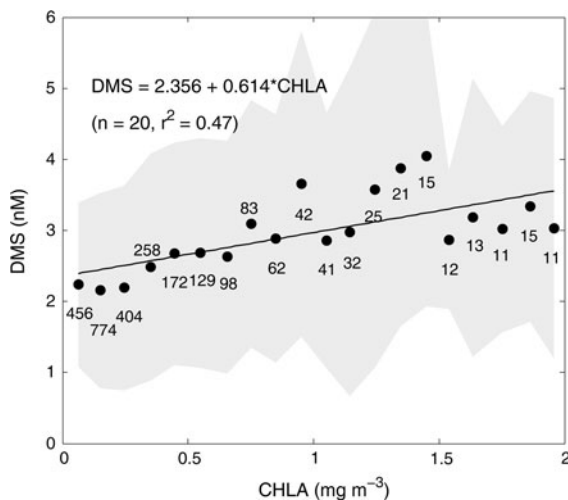


Fig. 6 Linear regression of DMS concentrations (L10 climatology) averaged by 10° latitude \times 20° longitude boxes against Chla concentrations binned in 0.1 mg m^{-3} intervals

box Chla concentration means binned into 0.1 mg m^{-3} intervals (Fig. 6). An upper limit of 2 mg m^{-3} was imposed onto the box Chla means to exclude the coastal and local phytoplankton blooms that carry extremely high values. The regression coefficient is low ($r^2 = 0.47$, $n = 20$) in agreement with the results of the distribution of the correlation between the two variables.

Conclusions

With the use of an increased number of DMS measurements and an updated global monthly climatology we have confirmed the salient features of the global monthly emerging patterns found in previous studies: (a) There is a general seasonal trend towards higher DMS concentrations in each hemispheric summer; (b) this seasonal pattern largely coincides with that of the daily solar radiation dose in the upper mixed layer of the ocean; (c) a proportionality between DMS and Chla only occurs north of 40°N and south of 40°S , while both variables are anti-correlated in most of the 40°N – 40°S latitudinal band. These emerging patterns could be illustrative of some of the factors that control the ocean's source of volatile sulfur for the Earth system. Due to the large uncertainties associated with the computation of global variables, the reported relationships have to be taken with caution and as

indicative of where further studies should be aimed to. In situ time series studies should be conducted to test these global emerging patterns, and the complexity of the interplay between physical, chemical, and biological processes that drive global DMS distributions should be investigated in process-oriented studies.

Acknowledgments The authors want to thank each of the individual contributors that generously submitted their DMS data to the Global Surface Seawater Dimethylsulfide Database, and to J.E. Johnson and T.S. Bates for the maintenance of the database. We thank M. Galí and the two reviewers for their helpful comments. We thank the Ocean Biology Processing Group at GSFC for the production and distribution of the monthly chlorophyll *a* data. This work was supported by the Spanish Ministry of Science and Innovation through the projects MIMOSA, PRISMA and Malaspina 2010, and through a PhD studentship to A.L.

References

- Anderson TR, Spall SA, Yool A, Cipollini P, Challenor PG, Fasham MJR (2001) Global fields of sea surface dimethylsulfide predicted from chlorophyll, nutrients and light. *J Mar Syst* 30(1–2):1–20
- Andreae MO, Crutzen PJ (1997) Atmospheric aerosols: biogeochemical sources and role in atmospheric chemistry. *Science* 276(5315):1052–1058
- Aumont O, Belviso S, Monfray P (2002) Dimethylsulfonylpropionate (DMSP) and dimethylsulfide (DMS) sea surface distributions simulated from a global three-dimensional ocean carbon cycle model. *J Geophys Res Oceans* 107(C4):3029. doi:[10.1029/1999JC000111](https://doi.org/10.1029/1999JC000111)
- Bates TS, Lamb BK, Guenther A, Dignon J, Stoiber RE (1992) Sulfur emissions to the atmosphere from natural sources. *J Atmos Chem* 14:315–337
- Bell TG, Poulton AJ, Malin G (2010) Strong linkages between dimethylsulfonylpropionate (DMSP) and phytoplankton community physiology in a large subtropical and tropical Atlantic Ocean data set. *Glob Biogeochem Cycles* 24:GB3009. doi:[10.1029/2009GB003617](https://doi.org/10.1029/2009GB003617)
- Belviso S, Moulin C, Bopp L, Stefels J (2004) Assessment of a global climatology of oceanic dimethylsulfide (DMS) concentrations based on SeaWiFS imagery (1998–2001). *Can J Fish Aquat Sci* 61(5):804–816. doi:[10.1139/F04-001](https://doi.org/10.1139/F04-001)
- Bopp L, Aumont O, Belviso S, Blain S (2008) Modelling the effect of iron fertilization on dimethylsulphide emissions in the southern ocean. *Deep-Sea Res Pt II* 55(5–7):901–912. doi:[10.1016/j.dsr2.2007.12.002](https://doi.org/10.1016/j.dsr2.2007.12.002)
- Brock TD (1981) Calculating solar radiation for ecological studies. *Ecol Model* 14(1–2):1–19
- Charlson RJ, Lovelock JE, Andreae MO, Warren SG (1987) Oceanic phytoplankton, atmospheric sulfur, cloud albedo and climate. *Nature* 326(6114):655–661
- Dacey JWH, Howse FA, Michaels AF, Wakeham SG (1998) Temporal variability of dimethylsulfide and dimethylsulfonylpropionate in the Sargasso Sea. *Deep-Sea Res Pt I* 45(12):2085

- Dasgupta S, Singh RP, Kafatos M (2009) Comparison of global chlorophyll concentrations using MODIS data. *Adv Space Res* 43(7):1090–1100. doi:[10.1016/j.asr.2008.11.009](https://doi.org/10.1016/j.asr.2008.11.009)
- de Boyer Montégut C, Madec G, Fischer AS, Lazar A, Iudicone D (2004) Mixed layer depth over the global ocean: an examination of profile data and a profile-based climatology. *J Geophys Res* 109:C12003. doi:[10.1029/2004JC002378](https://doi.org/10.1029/2004JC002378)
- Derevianko GJ, Deutsch C, Hall A (2009) On the relationship between ocean DMS and solar radiation. *Geophys Res Lett* 36:L17606. doi:[10.1029/2009GL039412](https://doi.org/10.1029/2009GL039412)
- Elliott S (2009) Dependence of DMS global sea-air flux distribution on transfer velocity and concentration field type. *J Geophys Res Biogeosci* 114:G02001. doi:[10.1029/2008JG000710](https://doi.org/10.1029/2008JG000710)
- Galí M, Saló V, Almeda R, Calbet A, Simó R (2011) Stimulation of gross dimethylsulfide (DMS) production by solar radiation. *Geophys Res Lett* 38:L15612. doi:[10.1029/2011GL048051](https://doi.org/10.1029/2011GL048051)
- Halloran PR, Bell TG, Totterdell IJ (2010) Can we trust empirical marine DMS parameterisations within projections of future climate? *Biogeosciences* 7:1645–1656. doi:[10.5194/bg-7-1645-2010](https://doi.org/10.5194/bg-7-1645-2010)
- Kettle AJ, Andreae MO (2000) Flux of dimethylsulfide from the oceans: a comparison of updated data seas and flux models. *J Geophys Res Atmos* 105(D22):26793–26808
- Kettle AJ, Andreae MO, Amouroux D, Andreae TW, Bates TS, Berresheim H, Bingemer H, Boniforti R, Curran MAJ, DiTullio GR, Helas G, Jones GB, Keller MD, Kiene RP, Leck C, Levasseur M, Malin G, Maspero M, Matrai P, McTaggart AR, Mihalopoulos N, Nguyen BC, Novo A, Putaud JP, Rapsomanikis S, Roberts G, Schebeske G, Sharma S, Simó R, Staubes R, Turner S, Uher G (1999) A global database of sea surface dimethylsulfide (DMS) measurements and a procedure to predict sea surface DMS as a function of latitude, longitude, and month. *Glob Biogeochem Cycles* 13(2):399–444
- Kiehl JT, Trenberth KE (1997) Earth's annual global mean energy budget. *B Am Meteorol Soc* 78(2):197–208
- Kiene RP, Kieber DJ, Slezak D, Toole DA, del Valle DA, Bisgrove J, Brinkley J, Rellinger A (2007) Distribution and cycling of dimethylsulfide, dimethylsulfoniopropionate, and dimethylsulfoxide during spring and early summer in the Southern Ocean south of New Zealand. *Aquat Sci* 69(3):305–319. doi:[10.1007/s00027-007-0892-3](https://doi.org/10.1007/s00027-007-0892-3)
- Lana A, Bell TG, Simó R, Vallina SM, Ballabrera-Poy J, Kettle AJ, Dachs J, Bopp L, Saltzman ES, Stefels J, Johnson JE, Liss PS (2011) An updated climatology of surface dimethylsulfide concentrations and emission fluxes in the global ocean. *Glob Biogeochem Cycles* 25(1):GB1004. doi:[10.1029/2010GB003850](https://doi.org/10.1029/2010GB003850)
- Le Clainche Y, Vecina A, Levasseur M, Cropp R, Gunson J, Vallina SM, Vogt M, Lancelot C, Allen I, Archer S, Bopp L, Deal C, Elliott S, Jin M, Malin G, Schoemann V, Simó R, Six K, Stefels J (2010) A first appraisal of prognostic ocean DMS models and prospects for their use in climate models. *Glob Biogeochem Cycles* 24:GB3021. doi:[10.1029/2009GB003721](https://doi.org/10.1029/2009GB003721)
- Locarnini RA, Mishonov AV, Antonov JJ, Boyer TP, Garcia HE, Baranova OK, Zweng MM, Johnson DR (2010) World Ocean Atlas 2009, volume 1: temperature. In: Levitus S (ed) NOAA Atlas NESDIS. 68. U.S. Government Printing Office, Washington DC, p 184
- Longhurst A (1998) Ecological geography of the sea. Academic Press, London
- Miles CJ, Bell TG, Lenton TM (2009) Testing the relationship between the solar radiation dose and surface DMS concentrations using in situ data. *Biogeosciences* 6:1927–1934
- Simó R (2001) Production of atmospheric sulfur by oceanic plankton: biogeochemical, ecological and evolutionary links. *Trends Ecol Evol* 16(6):287–294
- Simó R (2004) From cells to globe: approaching the dynamics of DMS(P) in the ocean at multiple scales. *Can J Fish Aquat Sci* 61(5):673–684. doi:[10.1139/F04-030](https://doi.org/10.1139/F04-030)
- Simó R, Dachs J (2002) Global ocean emission of dimethylsulfide predicted from biogeophysical data. *Glob Biogeochem Cycles* 16(4):1078
- Simó R, Pedrós-Alió C (1999) Role of vertical mixing in controlling the oceanic production of dimethyl sulphide. *Nature* 402(6760):396–399
- Six KD (2006) What controls the oceanic dimethylsulfide (DMS) cycle? A modeling approach. *Glob Biogeochem Cycles* 20(4):GB4011. doi:[10.1029/2005GB002674](https://doi.org/10.1029/2005GB002674)
- Stefels J (2000) Physiological aspects of the production and conversion of DMSP in marine algae and higher plants. *J Sea Res* 43(3–4):183–197
- Sunda W, Kieber DJ, Kiene RP, Huntsman S (2002) An antioxidant function for DMSP and DMS in marine algae. *Nature* 418(6895):317–320
- Toole DA, Siegel DA (2004) Light-driven cycling of dimethylsulfide (DMS) in the Sargasso Sea: closing the loop. *Geophys Res Lett* 31(9):L09308. doi:[10.1029/2004GL019581](https://doi.org/10.1029/2004GL019581)
- Vallina SM, Simó R (2007a) Strong relationship between DMS and the solar radiation dose over the global surface ocean. *Science* 315(5811):506–508. doi:[10.1126/science.1133680](https://doi.org/10.1126/science.1133680)
- Vallina SM, Simó R (2007b) Re-visiting the CLAW hypothesis. *Environ Chem* 4:384–387. doi:[10.1071/EN07055](https://doi.org/10.1071/EN07055)
- Vallina SM, Simó R, Gasso S (2006) What controls CCN seasonality in the southern ocean? A statistical analysis based on satellite-derived chlorophyll and CCN and model-estimated OH radical and rainfall. *Glob Biogeochem Cycles* 20(1):B1014. doi:[10.1029/2005GB002597](https://doi.org/10.1029/2005GB002597)
- Vallina SM, Simó R, Gasso S, de Boyer-Montégut C, del Rio E, Jurado E, Dachs J (2007) Analysis of a potential ‘solar radiation dose-dimethylsulfide-cloud condensation nuclei’ link from globally mapped seasonal correlations. *Glob Biogeochem Cycles* 21(2):B2004. doi:[10.1029/2006GB002787](https://doi.org/10.1029/2006GB002787)
- Vila-Costa M, Kiene RP, Simó R (2008) Seasonal variability of the dynamics of dimethylated sulfur compounds in a coastal northwest Mediterranean site. *Limnol Oceanogr* 53:198–211
- Vogt M, Vallina SM, Buitenhuis ET, Bopp L, Le Quere C (2010) Simulating dimethylsulphide seasonality with the dynamic green ocean model PlankTOM5. *J Geophys Res* 115:C06021. doi:[10.1029/2009JC005529](https://doi.org/10.1029/2009JC005529)